APPENDIX

PUBLICATIONS ARISING FROM THE DISSERTATION

Appendix A

Microstructure and transformation characteristics of a TiAlNb alloy with Cr and Mo addition

Santirat Nansaarng and Panya Srichandr

Materials Research Ibero-american Journal of Materials, 2012, Vol. 15, Issue 1, pp.63-69.

Materials Research. 2012; 15(1): 63-69
DOI: 10.1590/S1516-14392011005000095

Microstructure and Transformation Characteristics of a TiAlNb Alloy with Cr and Mo Addition

Santirat Nansaarng**, *Panya Srichandr

Division of Materials Technology, School of Energy, Environment and Materials, King Mongkut's University of Technology Thonburi (KMUTT), Bangkok, 10140, Thailand

Received: May 28, 2011; Revised: September 15, 2011

The present study investigated the Ti-46Al-4Nb-2Mo and Ti-46Al-4Nb-2Cr (at.%) alloys, which were prepared by solution treatment at 1,400 °C for 30 minutes prior to being air-cooled. The alloys were subsequently reheated to 1,350 °C for 60 minutes and were cooled to room temperature by oil or water quenching. The evolution of the microstructure in the alloys was investigated by detailed characterization of the massive-γ transformation of the heat-treated samples by optical microscopy and electron backscatter diffraction (EBSD). Lamellar structures consisting of and α_2 phases with small amounts of β-phase were distributed along the grain boundary after the solution treatment process in both alloys. A massive-γ transformation from the α-phase field was observed for the samples that were cooled by water or oil quenching. After cooling in either oil or water, the massive-γ transformed structure of Ti-46Al-4Nb-2Cr without a lamellar phase was distributed on the α_2-matrix. In addition, the massive-γ phases confirmed that the nucleation site was at the grain boundary of the α/α parent phase. Moreover, the volume fraction of massive-γ decreased as the cooling rate increased. The EBSD results demonstrated that the massive-γ transformation inherited the orientation of the lamellar-γ, and nucleation occurred around the parent α-matrix. The detailed observation orientation relationship by Kikuchi patterns and pole figures revealed a massive- transformation, and the α_2-matrix had the associated orientation relationship from the γ-lamellar and parent α-matrix.

Keywords: *massive-γ, EBSD technique, phase transformation, alloying elements, heat treatment*

1. Introduction

Titanium aluminides are potential candidates for structural high-temperature components, particularly in aerospace and automotive applications, because of their low density, high melting temperature, high specific tensile strength, strength at elevated temperatures and strong oxidation resistance[1-3]. Titanium aluminides, however, have lower formality, and the production and forming processes are technically difficult. Among the titanium aluminides, the γ-TiAl alloy group is the most popular for industrial services because the two-phase structure between α_2(Ti_3Al) and γ(TiAl) results in improved mechanical properties. The microstructure and mechanical properties of TiAl alloys are strongly influenced by both the chemical composition and the heat-treatment procedures employed. Regarding the chemical composition, alloying with a ternary or quaternary element (e.g., Nb, Mo, Cr, V, B, or Si) can have significant effects on the microstructure and the mechanical properties of the alloys[4,5]. The microstructure is ultimately controlled by the heat treatment, and the cooling rate is particularly important in determining the microstructure of titanium aluminides because phase transformation mechanisms control the final nature of the microstructure[6]. Studies by Wu et al.[7,8] found that improvements in the mechanical properties of cast titanium aluminides were due to the effects of the casting process on the microstructure. Indeed, massive-γ phases can be formed from a single α-phase field by a partitionless transformation, which is initiated by varying the cooling rate. Studies have also shown that the addition of alloying elements, such as Nb, Mn[9] and Ta[10], have a greater effect on the transformation because they increase the effective range of cooling rates and promote massive-γ formation. Many studies have investigated the phase transformation mechanisms for the α-phase (at high temperatures) transformation to the α_2 and γ-lamellar form or to massive-γ. Interestingly, two massive transformation processes have received considerable attention for refining the microstructure and improving the mechanical properties of casting products[7]. Several previous studies have focused on the ternary composition, the nucleation process, and the orientation relationship between the parent α-phase and the product massive-γ phase[7,9]. In addition, alternative techniques, such as the EBSD technique, have explored the nucleation mechanism of the massive transformed-γ phase to explain phase orientation that is developed at the α/α parent phase grain boundary and through orientation between lamellar structure and massive structure[11]. The aim of the present work was to study the effect of alloying elements (e.g., Nb, Mo, and Cr) and the cooling rate on the massive-γ phase transformation and phase characteristics of TiAl alloys (Ti-46Al-4Nb-2Mo and Ti-46Al-4Nb-2Cr) using the EBSD technique.

*e-mail: santirat.nan@kmutt.ac.th

2. Materials and Methods

Ti-46Al-4Nb-2Mo and Ti-46Al-4Nb-2Cr (at. %) alloys were prepared using the non-consumable vacuum arc melting technique in an argon atmosphere. Button ingots that weighed approximately 60 g were re-melted at least five times to ensure the homogeneity of the chemical composition. Samples were cut from the as-cast buttons by wire-electrical-discharge machining. Next, the samples were solution-treated by soaking at the temperature of the α single-phase area (1,400 °C) for 30 minutes and subsequently air-cooled (AC). Next, the solution-treated samples (nominal dimensions of 10 × 10 × 10 mm) were heat-treated at 1,350 °C for 60 minutes and quenched in either oil quenching (OQ) and water quenching (WQ), which produces different microstructures.

All of the heat-treated samples were abraded with SiC-based emery paper to remove the oxidized surface layer, rinsed with water, polished to a 0.1-μm finish with a diamond suspension abrasive, and etched using Kroll's regent (5 mL HF, 10 mL HNO_3, and 85 mL H_2O). The microstructures and resultant phases in the heat-treated samples were studied using X-ray diffraction (XRD), an optical microscope with a Leica Q-Phase image analyzer, scanning electron microscopy (SEM), back-scattered electron detection (BSE) and electron backscatter diffraction (EBSD).

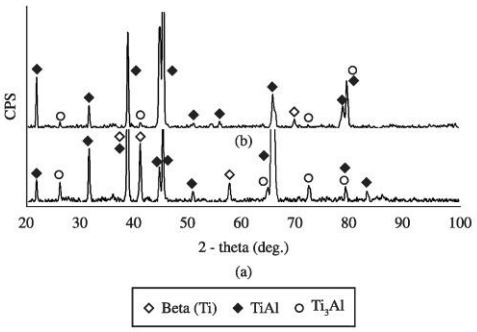

Figure 1. X-ray diffraction patterns of the two alloys in as-received condition revealed three phases: γ, α_2 and β phases. a) Ti-46Al-4Nb-2Mo, and b) Ti-46Al-4Nb-2Cr.

3. Results

3.1. *Solution treatment*

Figure 1 shows the XRD patterns of Ti-46Al-4Nb-2Mo and Ti-46Al-4Nb-2Cr samples in as-received condition (that is, solution-treated at 1,400 °C for 30 minutes and air-cooled). The diffraction peaks confirmed that the alloys primarily consisted of the γ-TiAl phase with minor amounts of the α_2-Ti_3Al phase and the β phase. The optical micrographs showed a typical lamellar microstructure, which consisted of alternate layers of γ, α_2 and β phases. There was a small volume fraction of equiaxed regions within the lamellar structure of the Ti-46Al-4Nb-2Mo and Ti-46Al-4Nb-2Cr alloys (Figure 2a and 2b). The equiaxed microstructure of the Ti-46Al-4Nb-2Cr alloy sample more pronounced than the other samples (approximately 20% equiaxed structure). The BSE images of both the Ti-46Al-4Nb-2Mo and Ti-46Al-4Nb-2Cr alloys (Figure 3a and 3b) showed evidence of the β phase along the colony boundaries and distributed in the lamellar-γ matrix.

3.2. *Microstructures*

Representative optical micrographs of Ti-46Al-4Nb-2Mo and Ti-46Al-4Nb-2Cr samples directly quenched using either oil or water from 1,350 °C are shown in Figure 4. In addition, Figures 4a-d also show the structure of the massive-γ transformation on the matrix of α_2 and its distribution over the area of the cross section, which is different from the structure observed in the solution-treated samples where the massive-γ structure was not found. Interestingly, we found that the Ti-46Al-4Nb-2Mo sample had significantly more massive- structure than did the Ti-46Al-4Nb-2Cr sample. In the microstructure of

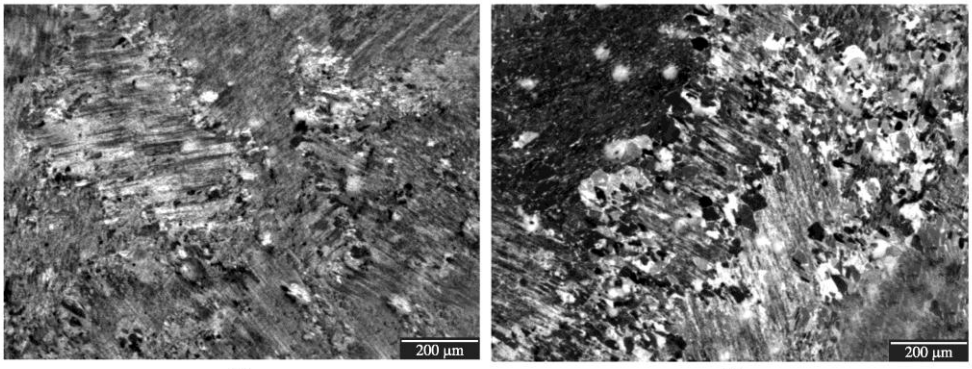

(a) (b)

Figure 2. Microstructure of the as-received condition, which shows the lamellar and equiaxed structure of: a) Ti-46Al-4Nb-2Mo, and b) Ti-46Al-4Nb-2Cr.

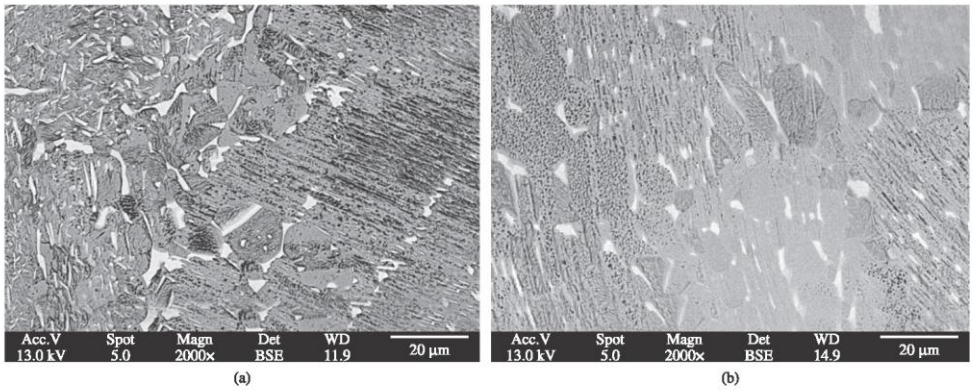

Figure 3. BSE images of the β-phase (bright field) of the two alloys in as-received condition, which shows the β-phase distributed along the grain boundary in: a) Ti-46Al-4Nb-2Mo, and b) Ti-46Al-4Nb-2Cr.

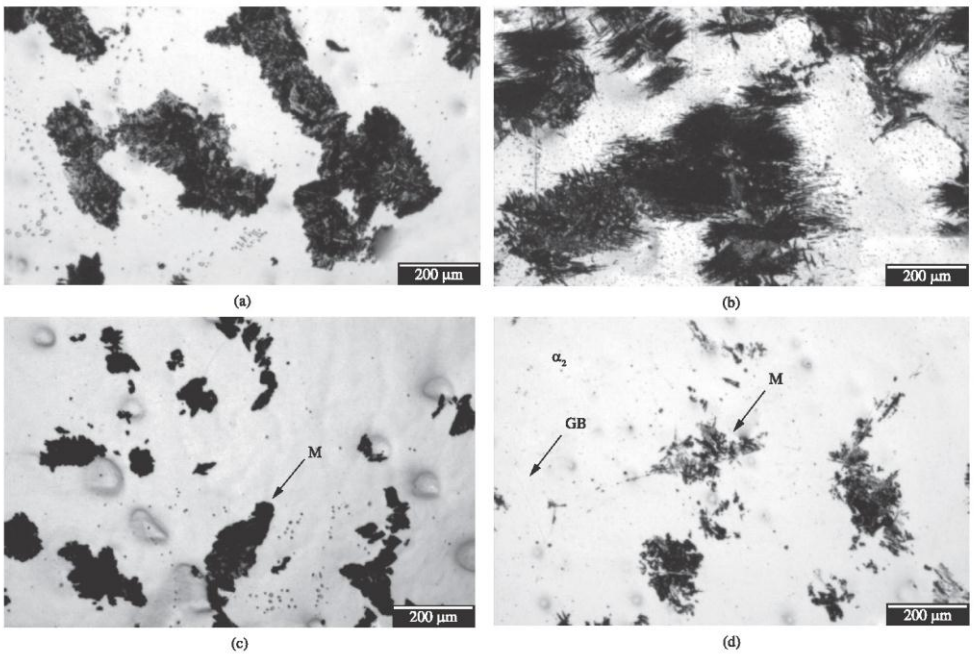

Figure 4. Micrographs of Ti-46Al-4Nb-2Mo and Ti-46Al-4Nb-2Cr oil and water quenched from 1,350 °C. All samples showed a massive-γ transformed phase (M) that resembled a small island (dark) distributed on an α_2- matrix (bright): a,c) show microstructures of Ti-46Al-4Nb-2Mo cooled by oil and water quenching, respectively, b,d) show microstructures of Ti-46Al-4Nb-2Cr cooled by oil and water quenching, respectively.

Ti-46Al-4Nb-2Mo with OQ cooling, the massive-γ phase distribution was present in the α_2-matrix. These massive-γ phase regions look similar to small islands (dark) that surround the α_2-matrix, but the nucleated site is not clear because we could not find the grain boundary (Figure 4a, which had a volume fraction of approximately 45%). The microstructure of Ti-46Al-4Nb-2Cr (Figure 4b) was large-grained and mainly consisted of colonies of massive-γ + α_2 phase (the massive-γ colony size was approximately 350-500 µm). The nucleation of massive-γ was transformed at the grain boundary, and there was subsequent growth into the grain. The microstructures of Ti-46Al-4Nb-2Mo cooled by WQ, however, revealed a massive-γ structure (dark in appearance) on the α_2-massive matrix (light in appearance)

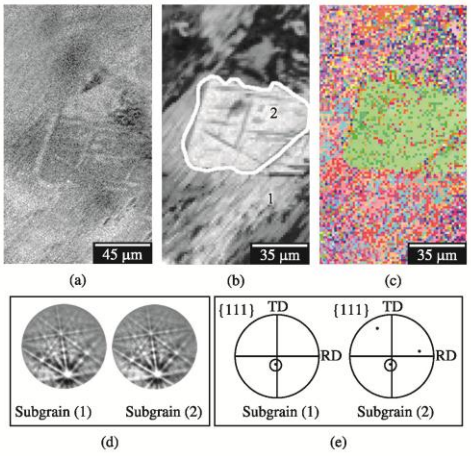

Figure 5. Micrographs and diffraction patterns from a sample of Ti-46Al-4Nb-2Mo oil quenched from 1,350 °C. a) A backscattered scanning electron micrograph image, and b) an EBSD image showing that the massive-γ was associated with gamma in the lamellae form (subgrain 1). c) An EBSD image showing different colored areas. d) Kikuchi maps, and e) pole figures of massive-γ and lamellar structure marked as subgrains 1 and 2 show that they have identical orientation, which suggests that subgrain 1 was the formation of the twin-related to subgrain 2.

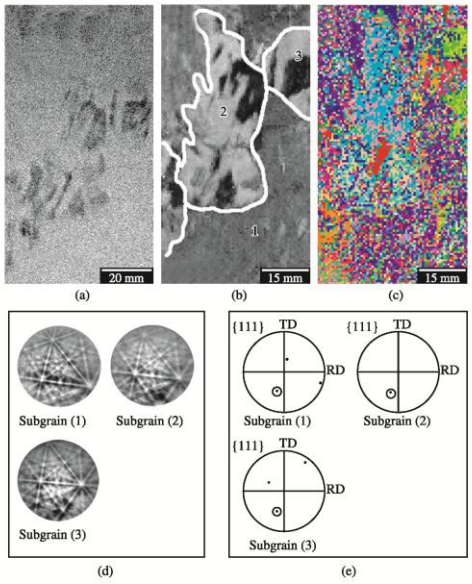

Figure 6. Micrographs and diffraction patterns from a sample of Ti-46Al-4Nb-2Cr oil quenched from 1,350 °C. a) A backscattered scanning electron micrograph image, and b) an EBSD image showing the difference between the two regions with dark and light areas, which indicate the occurrence of massive-γ. c) An EBSD image, d) Kikuchi maps, and e) pole figures of subgrains 1, 2 and 3 show that the the massive-γ transformed structure within subgrains 2 and 3 was nucleated from twin-related to subgrain 1 with the (111) plane.

with an approximately 21% volume fraction of massive-γ phase (Figure 4c). For the Ti-46Al-4Nb-2Cr alloy, the microstructures consisted of a featureless bright α_2-matrix with fine acicular patches of massive-γ structure dispersed on the matrix. In addition, nucleation appeared to start at the α_2 grain boundaries (colony size ~ 30-200 µm). The volume fraction of this massive-γ phase was approximately 15% (Figure 4d).

The EBSD results from the Ti-46Al-4Nb-2Mo sample quenched by oil are shown in Figure 5. The backscattered image in Figure 5a and the EBSD image in Figure 5b show that the massive-γ transformation was associated with gamma in the lamellar-γ form. The EBSD image in Figure 5c shows that there were different orientations between the lamellar-γ (labeled 1) and massively transformed-γ (labeled 2) regions. When considering the two regions in the image, it was determined that they were not associated with orientation. Importantly, the Kikuchi maps shown in Figure 5d confirmed that the massive-γ in subgrain 2 had the same orientation as the lamellar-γ in subgrain 1. The stereograms in Figure 5e revealed information about the involvement of subgrain 1 and subgrain 2, and we determined that subgrain 1 was related to subgrain 2; thus, the twin phenomenon, which was reported by S.R. Dey et al.[11], was confirmed. Indeed, the growth of the massive structure was created from the low-stacking-fault energy and the nucleated twinning over the {111} plane.

The EBSD image in Figure 6a shows the massive-γ structure of the Ti-46Al-4Nb-2Cr OQ sample. Figure 6b shows the difference between the two regions with dark and light areas, which indicate the occurrence of massive-γ. The EBSD image in Figure 6c explains the orientation relationships as subgrain 1, subgrain2 and subgrain 3. The overall results of the microstructures in the three subgrains revealed the massive-γ transformed structure. The orientation relationships of all three subgrains from the Kikuchi maps shown in Figure 6d confirmed that the massively transformed structure within subgrain 2 and subgrain 3 were nucleated from twin-related regions in subgrain 1 in the (111) plane. The orientation relationships were also confirmed by the pole figure in Figure 6e.

Figure 7 shows the microstructure of Ti-46Al4Nb-2Mo cooled by WQ. The EBSD images in Figures 7a-c show the components of the lamellar structure (region 1) and massive-γ structure (region 2). These finding is apparently from the color region in the EBSD image and from the associated pole figures and corresponding Kikuchi maps shown in Figures 7c-e. The Kikuchi maps shown in Figure 7d confirm that the massive-γ in region 2 has the identical orientation with lamellar in region 1. The stereograms in Figure 7e from the lamellar and massive-γ region, show that the massive-γ in region 2 is parallel with a (111) in region 2 and twin-related to region 1 with (111) plane.

Samples of Ti-46Al-4Nb-2Cr quenched in water exhibited massive-γ transformation (Figures 8a-d). The microstructure of the Ti-46Al-4Nb-2Cr sample showed a

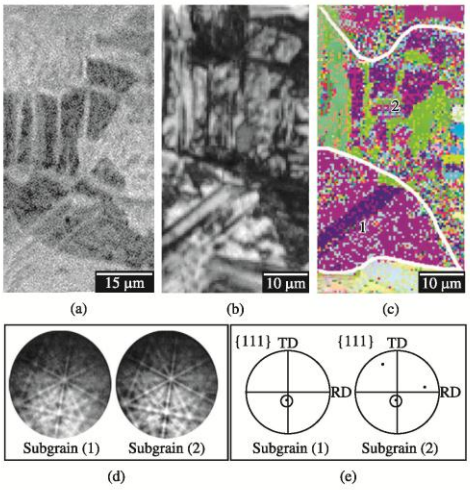

Figure 7. Micrographs and diffraction patterns from a sample of Ti-46Al-4Nb-2Mo water quenched from 1,350°C. a) A backscattered scanning electron micrograph image, and b) an EBSD image showing that the massive-γ was associated with gamma in the lamellae form (subgrain 1). c) An EBSD image, d) Kikuchi maps, and e) pole figures of subgrains 1 and 2 show the Kikuchi maps taken from regions 1 and 2 and the poles to the {111} plane. The two regions have the same orientation, and region 2 was twin-related to region 1.

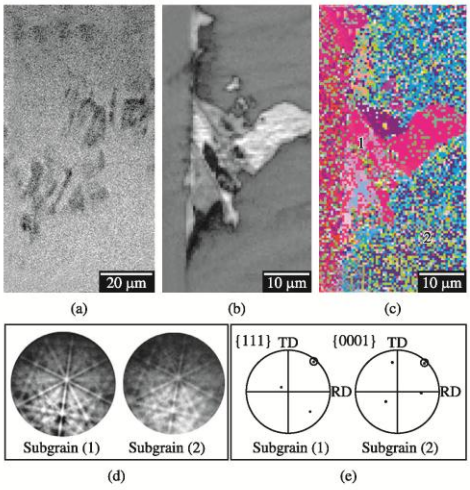

Figure 8. Micrographs and diffraction patterns from a sample of Ti-46Al-4Nb-2Cr water quenched from 1,350°C. a) A backscattered scanning electron micrograph image, and b) an EBSD image showing that massive-γ was nucleated at the grain boundary and grew into the parent phase (like a small island). c) An EBSD image, d) Kikuchi maps, and e) pole figures of subgrains 1 and 2 show that the massive-γ was nucleated at the grain boundary and grew into the parent phase (resembling a small island). In addition, more structure contrast was seen in the two regions, and the association between the massive-γ (region 1) and the alpha parent phase (region 2) had the same orientation. Indeed, the relationship between the matrix (0001) of the alpha phase was parallel with (111) plane in the massive-γ.

similar transformation as the previous case (Ti-46Al4Nb-2Mo cooled by WQ); however, the Ti-46Al-4Nb-2Cr sample showed a clear nucleation site of the massive-γ formation. Figure 8b shows that the massive-γ was nucleated at the grain boundary and grew into the parent phase (as a small island). In addition, there was more structure contrast in the two regions. The {111} pole figure and Kikuchi maps from Figures 8d and e show that the massive-γ (region 1) and alpha parent phase (region 2) had the same orientation relationship. Indeed, the matrix (0001) of the alpha parent phase was parallel with the (111) plane in region 1 of the massive-γ.

Although samples were cooled down using different media (i.e., oil or water), the relationship between the matrix structure, alpha phase and massive-γ of the samples indicated that the structural transformation was the same in each composition. Alloying with Mo and Cr, however, resulted in different microstructures. The addition of Cr could clearly be observed for the massive transformation because the microstructure revealed the massive-γ and alpha parent phase without the lamellar structure (Figures 6 and 8).

4. Discussion

The different amounts of alloying elements selected in the present study resulted in phase transformations at temperatures greater than the eutectoid temperature by subsequent quenching in two different media (i.e., oil and water). The microstructures of samples formed by solution treatment showed that both alloys had two types of structure (i.e., full lamellar and small random regions of equiaxed α_2 phase and phase). The Ti-46Al-4Nb-2Mo had a finer colony size than the Ti-46Al-4Nb-2Cr alloys; however, the Ti-46Al-4Nb-2Cr alloy exhibited the highest volume fraction of transformed equiaxed microstructure at the grain boundaries. Sreenivasulu et al.[5] reported that decreasing Nb and increasing Mo increased the volume fraction of transformed equiaxed microstructures compared with Ti-46Al-4Nb-2Cr; therefore, the kinetics of lamellar to equiaxed transformation are decreased by Nb and increased by Mo. The addition of Mo resulted in increased stability in the β phase. The BSE images revealed that Mo more strongly segregated the β phase compared with Nb and Cr (Figure 3a and 3b). Imayev et al.[12] confirmed that Nb and Mo effectively improve the kinetically stabilized β phase along the α grain boundaries and hinder the growth of α grains passing through the α single-phase field. Indeed, the addition of Mo expands the β phase region toward the α-phase and γ-phase regions in the isothermal section of the ternary phase system[13]. When heat-treated, diffusion of Mo and Al occurs in opposite directions, which tends to equilibrate these gradients, and zones of microstructure exist, depending upon the extent to which diffusion has occurred. Interestingly, alloys with Cr and Mo addition from both the as-cast condition and after heat treatment demonstrated that alloying solidification happened in a single-phase β region. Although segregation existed within

the β grains (forming a complete solidification stage), the composition gradients were not notably strong, and the structures seen within the β grains were uniform. The distribution of β phases was dominated by the primary post-solidification transformation, which resulted in the formation of a lath in the Mo-lean alloys and γ plates that directly formed from the β phase in the Mo-rich alloys[14].

In the two investigated alloys that were subjected to solution treatments and cooled by oil and water quenching, we found that the phase transformations resulted in the same microstructures (i.e., massive-γ with an α_2-matrix). Interestingly, the addition of Cr had a greater effect on the massive transformation; however, the Mo alloys had a massive structure with some lamellar structures. When comparing the effect of quenching media on the quantity of massive structure formed, the volume fraction of massive-γ formed by oil quenching was greater than by water quenching for both Ti-46Al-4Nb-2Mo and Ti-46Al-4Nb-2Cr. Because Nb has a low diffusivity in TiAl alloys, the formation of diffusion-related feathery/lamellar transformations is suppressed, which allows massive transformation to occur[10]. The addition of Nb also extends the massive regime in TiAl alloys toward rapid cooling rates observed between oil and water quenching. The addition of Mo and Cr in TiAl alloys was found to form similar feather-type microstructures as with the massive-γ formed in both oil and water quenching.

The massive-γ transformation mechanism has proved difficult to explain. The observation of the nuclei of the massive formation has been especially difficult to explain because the massive-γ structure can nucleate from the lamellar structure above the usual massive transform temperature[15]. In addition, the massive-γ structures can nucleate from single atom jump diffusional α→γ phase transformations and spread in all directions with no large-scale composition change[16]. Some proposed mechanisms have indicated that the transformation to massive-γ occurs because of a twinning mechanism between the massive transformation processes. Thus, one strategy that can be used to consider massive transformation phenomenon is to observe the formation of twins in the (111) plane because this plane is the site of nucleation of massive-γ. If the twinning occurred at this point, the relationship could reveal the orientation between the massive transformation and the alpha matrix[11]. In the present study, we found that the massive-γ formation was relevant to the alpha parent phase in all alloys with either water or oil quenching. The orientation relationship in this study was found to indicate that same orientation with {111}γ//{0001}α, which is confirmed in Figures 5-8 (panel d in all figures). The probability mechanism that which could explain the relationship of the orientation in this study was the formation of massive-γ. This massive-γ transform was nucleated at the longitudinal grain boundary of the prior α/α grain, which confirmed this massive transformation mechanism (Figure 8). Although the initial nucleus may be coherent, twinning that occurred on the {111} plane, which is not the original interface, would result in a massively transformed gamma that no longer had a simple orientation relationship with the alpha matrix[7]. The formation of massive-γ is clearly explained in earlier publications [e.g., References 7,8] that identified a competition between the growth of lamellae and the growth of massive-γ under the cooling conditions that were used to refine the microstructures. The results of all cooling rates with the two compositions (i.e., Ti-46Al-4Nb-2Mo and Ti-46Al-4Nb-2Cr) found that the alloy with the Cr addition as the quaternary alloying element promoted a massive transformed mechanism that was greater than the Mo addition; however, Mo promoted a greater formation of lamellar structure compared with Cr[17]. The use of Nb as the alloying element generally slows down the formation of lamellar microstructures, which implies that Nb may be related to its low diffusivity, and Nb is a slow diffuser in both TiAl and Ti_3Al. Indeed, Nb has a diffusion coefficient that is approximately an order of magnitude lower than that of Ti[18,19]. Interestingly, Cr is also a slow diffuser in both TiAl and Ti_3Al similar with Nb[18]. Thus, Nb and Cr both effectively extend the massive regime of the nucleated massive-γ transformation of Ti-46Al-4Nb-2Cr more than in Ti-46Al-4Nb-2Mo. Interestingly, we found that increasing the quenching rate (from OQ to WQ) led to a reduction in the volume fraction of massive-γ for all of the compositions, which confirmed the results of previous research [e.g., Reference 16].

5. Conclusions

1. The presence of Mo in the TiAlNb alloys affected the quantity of the β phase and facilitated the stability of the lamellar structures. Ti-46Al-4Nb-2Mo in as-received form had the highest volume fraction of β phase.
2. EBSD revealed that adding Mo and Cr affected the occurrence of massive-γ, and the addition of Cr improved the nucleation and growth of massive- more than the addition of Mo. In addition, the massive-γ transformation occurred without forming lamellar structure in alloys with the addition of Cr.
3. The massive-γ transformed phase was nucleated at the α-parent phase grain boundary and grew with the associated orientation relationship with the α-parent phase matrix that was inherited from twinning during transformation.
4. Increasing the cooling rate decreased the volume fraction of massive-γ structure.

References

1. Wu X. Review of alloy and process development of TiAl alloys. *Intermetallics*. 2006; 14 (10-11):1114-1122. http://dx.doi.org/10.1016/j.intermet.2005.10.019
2. Yamaguchi M, Inui H and Ito K. High-temperature structural intermetallics. *Acta Materiallia*. 2000; 4(1):307-322. http://dx.doi.org/10.1016/S1359-6454(99)00301-8
3. Apple F and Wagner R. Microstructure and deformation of two-phase γ-titanium aluminides. *Materials Science and Engineering*: R. 1998; (22):187-268.
4. Kim YW. Gamma titanium aluminide: their status and future. *JOM*. 1995; 47(7):39.
5. Sreenivasulu G, Singh AK, Mukhopadhyay NK and Sastry GVS. Effect of alloying and aging on morphological changes from lamellar to equiaxed microstructure of α_2+ γ titanium aluminides. *Metallurgical and Materials Transactions A*. 2001; 36(10):2603-2607.
6. Leonard KJ and Vasudevan VK. Phase equilibria and solid state transformations in Nb-rich Nb-Ti-Al intermetallic alloys. *Intermetallics*. 2000; 8(9-11):1257-1268. http://dx.doi.org/10.1016/S0966-9795(00)00056-X
7. Wu X, Hu D, Loretto MH and Huang AJ. The influence of interrupted cooling on the massive transformation in Ti46Al8Nb. *Intermetallics*. 2007; 15(9):1147-1155. http://dx.doi.org/10.1016/j.intermet.2007.02.002
8. Wu X, Saage H, Huang AJ, Hu D and Loretto MH. Microstructures and tensile properties of massively transformed and aged Ti46A18Nb and Ti46A18Ta alloys. *Intermetallics*. 2009; 17(1-2):32-38. http://dx.doi.org/10.1016/j.intermet.2008.09.006
9. Prasad U and Chaturvedi MC. Influence of alloying elements on the kinetics of massive transformation in gamma titanium aluminides. *Metallurgical and Materials Transactions A*. 2003; 34(10):2053-2066. http://dx.doi.org/10.1007/s11661-003-0270-2
10. Hu D, Huang AJ and Wu X. On the massive phase transformation regime in TiAl alloys: The alloying effect on massive/lamellar competition. *Intermetallics*. 2007; 15(3):327-332. http://dx.doi.org/10.1016/j.intermet.2006.07.007
11. Dey SR, Bouzy E and Hazotte A. EBSD characterisation of massive γ nucleation and growth in a TiAl-based alloy. *Intermetallics*. 2006; 14(4):444-449. http://dx.doi.org/10.1016/j.intermet.2005.08.010
12. Imayev RM, Imayev VM, Oehring M and Appel F. Alloy design concepts for refined gamma titanium aluminide based alloys. *Intermetallics*. 2007; 15(4):459. http://dx.doi.org/10.1016/j.intermet.2006.05.003
13. Kimura M and Hashimoto K. High-temperature phase equilibria in Ti-AI-Mo system. *Journal of Phase Equilibria*. 1999; 20(3):228.
14. Singh AK and Banerjee D. Transformations in α_2+ γ titanium aluminide alloys containing molybdenum: Part II. Heat treatment. *Metallurgical and Materials Transactions A*. 1997; 28(9):1745-1753. http://dx.doi.org/10.1007/s11661-997-0106-6
15. Zhung XD, Godfrey S, Weaver M, Strangwood M, Kaufman MJ and Loretto MH. The massive transformation in Ti-Al alloys: Mechanistic observations. *Acta Materiallia*. 1996; 44(9):3723. http://dx.doi.org/10.1016/1359-6454(95)00453-X
16. Veeraraghavan D, Wang P and Vasudeven VK. Kinetics and thermodynamics of the $\alpha \rightarrow \gamma_m$ massive transformation in a Ti-47.5 at.% Al alloy. *Acta Materiallia*. 1999; 47(11):3313-3330. http://dx.doi.org/10.1016/S1359-6454(99)00195-0
17. Yun JH, Oh MH, Nam SW, Wee DM, Inui H and Yamaguchi M. Microalloying Effects in TiAl+Mo Alloys. *Materials Science and Engineering*: A. 1997; 230-240:702-708.
18. Herzig Chr, Przeorski T, Friesel M, Hisker F and Divinski S. Tracer solute diffusion of Nb, Zr, Cr, Fe, and Ni in γ-TiAl: effect of preferential site occupation. *Intermetallics*. 2001; 9(6):461-472. http://dx.doi.org/10.1016/S0966-9795(01)00025-5
19. Mishin Y and Herzig C. Diffusion in the Ti-Al system. *Acta Materiallia*. 2000; 48(3):589-632. http://dx.doi.org/10.1016/S1359-6454(99)00400-0

Appendix B

Influence of Nb and Mo addition on Microstructure of Ti-46Al intermetallics alloys

Santirat Nansaarng and Panya Srichandr

Proceeding of the 7th International Materials Technology Conference and Exhibition,
IMTCE 2010 INOVATION FOR SUSTAINABILITY, 13-16 June 2010,
Hilton Kuching, Sarawak, Malaysia

Influence of Nb and Mo addition on Microstructures of Ti-46Al intermetallic alloys

Santirat Nansaarng[1], Panya Srichandr[1]
[1]Division of Materials Technology, School of Energy, Environment and Materials
King Mongkut University of Technology Thonburi, Bangkok 10140, Thailand.

Abstract

Two alloys, Ti-46Al-2Mo and Ti-46Al-4Nb-2Mo were prepared by non-consumable vacuum arc melting technique under an argon atmosphere. Treatment of all alloys was carried out using two steps, solution treatment and subsequent treatment. The solution treatment was by air cooling starting from the surface temperature at 1400°C for 30 min and subsequent treatment was by reheating alloys at 1350 °C for 1 h before cooling in various media such as furnace and water. The effect of processing and heat treatment on the two alloy microstructures were studied by X-ray diffractometry, optical microscopy, and scanning electron microscopy. The results showed that the solution-treatment alloys with a duplex microstructure consisted of lamellar colonies, and equiaxed γ phase with α_2 phases and β phase. Moreover, utilization of the slow cooling media such as furnace resulted in the increases of lamellar transformation kinetics while the increase of massive γ transformation kinetics were when used the rapid cooling media such as water quenching. Finally, addition of Nb and Mo significantly reduced colony size and promoted the massive transformation of TiAl alloys.

Keywords: keyword(s) γ-TiAl; TiAl alloys; two-phase structures; alloying elements; heat treatment

Introduction

Titanium aluminides was light alloys for high temperature in area of aerospace and automotives applications. Microstructural modifications and addition of ternary or fourthly elements are extensively used to optimize mechanical and oxidation properties of γ-based titanium aluminides. The addition of ternary or more elements and heat-treatment process are generally aimed at improving mechanical and oxidation properties necessary for high temperature application of these intermetallics [0]. The fine microstructures of fully two phases ($\alpha_2+\gamma$) lamellar as well as on the best of mechanical properties. Fully lamellar phase show evidence of good creep properties, fractures toughness, fatigue resistance and high temperatures strength [2-3]. The present study wills the microstructures of two alloys containing different alloying elements (Nb and Mo) and cooling rate (Furnace and water cooled), examining the microstructures morphology and phases characteristics.

Experimental procedure

The comparative study was carried out in two alloys, Ti-46Al-2Mo and Ti-4Al-4Nb-2Mo (at.%) were initially processed by non-consumable vacuum arc melting technique in argon atmosphere. Bottom ingots, approximately 60 g, were cut from the as-cast pancakes by EDM-wire cut and then solution treating, which soaking at the temperature of α single phase area (1400°C) for 30 min. and cooled by air. Solution treated samples with a dimension of 10 mm ×10 mm ×10 mm were subsequently heat-treated at 1350 °C for 1 h before performing cooling step. Different kinds of media were utilized in the cooling, selecting based on cooling speeds as the lowest cooling rate by furnace cooling (FC) and

[1] **Santirat Nansaarng:** Corresponding author, E-mail : santirat.nan@kmutt.ac.th, Phone +662-470-8554-6, Fax. +662-470-8557.

the fast cooling rate by water quenching (WQ). All alloy samples that have been heat-treated were ground with SiC-based emery paper in order to remove the oxidized layer from the exposed surface before rinsing with water, then polishing to a 0.1 μm finish with diamond suspension, and etching by Kroll's reagent (5HF, 10mL HNO_3, and 85mL H_2O). The microstructures and resultant phases of heat-treated samples were examined using X-ray diffraction (XRD), an optical microscope (OM) with Leica Q-Phase image analyzer, and a scanning electron microscope (SEM).

Results and Discussion

1. Solution treated conditions

Fig. 1 shows the XRD patterns of Ti-46Al-2Mo and Ti-46Al-4Nb-2Mo samples prepared from as-received condition (solution treatment at 1400 °C, 30 min, and air cooling). The results of the diffraction peak patterns indicated that the both alloys primarily consisted of the γ-TiAl phase with a minor amount of α_2-Ti_3Al phase and β phase. The optical micrographs also confirmed the results observed in the XRD pattern, presenting that a typical lamellar microstructure composed of alternate layers of γ, α_2, and β phases. Inside the lamellar structure of two alloy (Ti-46Al-2Mo and Ti-46Al-4Nb-2Mo), a small volume fraction of equiaxed regions was observed (Fig.2 (a) - (b) respectively). However, when compared microstructures between two alloys it was found similar microstructures contained equiaxed microstructure, as evidenced by the volume fraction of only around 20 pct equiaxed structure. Detailed observation of the BSE images of two alloys shown in Fig. 3 (a) - (b) revealed that the β phase was forming along colony boundaries and distributing on the γ matrix.

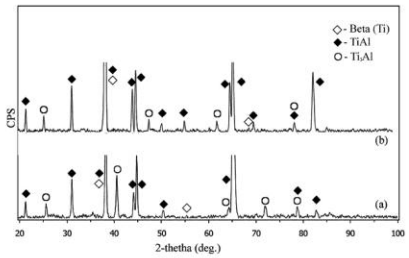

Fig.1. X-ray diffraction pattern of some alloys in as-receive: (a) Ti-46Al-2Mo, (b) Ti-46Al-4Nb-2Mo

2. Microstructures vs. cooling rate

After heat-treated at 1350°C, 1 h, the alloys were cooled at different rates. Figs.4 to 5 is the micrographs of all alloy microstructures cooled by various media. The slowest cooling rate received from using furnace, yielding the microstructures of the ternary alloys, Ti-46Al-2Mo composing of coarse α_2 + γ lamellar grains with the grain size (GS) of about 200-600 μm (Fig. 4(a)). However, the addition of the fourth element (Nb) to the Ti-46Al-2Mo alloys resulted in the decreases of α_2 + γ lamellar GS with GS at about 50 – 200 μm and 100 – 300 μm, respectively, and occurrence of some equiaxed γ-monolithic grains (Fig. 5(b)). Although the microstructures of Ti-46Al-2Mo and Ti-46Al-4Nb-2Mo alloys had finer colony sizes, they exhibited the highest volume fractions of equiaxed microstructure transformation at grain boundaries. Sreenivasulu et al.[4] reported that addition of Nb and Mo to alloying compositions can increase and decrease the volume fraction of transformation of equiaxed microstructures, respectively, implying that the Nb addition leads into decreasing of the transformation kinetic and adding of Mo results in the increase of kinetic. Moreover, the results from

BSE images demonstrated that addition of Mo to the alloy can cause β phase segregation more than those of Nb and Cr (Fig. 3(a) and (b), and this segregation results in increasing of the β phase stability. This finding is consistent with the report of Imayev et al.[5], describing that the higher partition coefficient $k_{\beta/\alpha}$ of Nb and Mo have strong effect on improving of the kinetically stabilized β phase along the α grain boundaries and hindering of the α grain growth passing through the α single-phase field. Thus, the Mo addition leads into expansion of the β phase region toward the α phase and γ phase regions in the isothermal section of the ternary phase system [6].

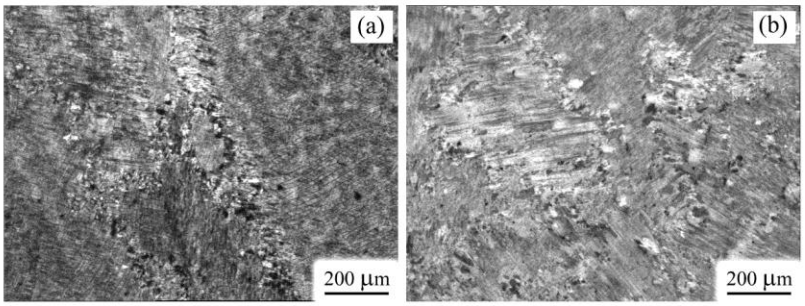

Fig.2 The microstructures of as-receive condition of (a) Ti-46Al-2Mo, (b) Ti-46Al-4Nb-2Mo

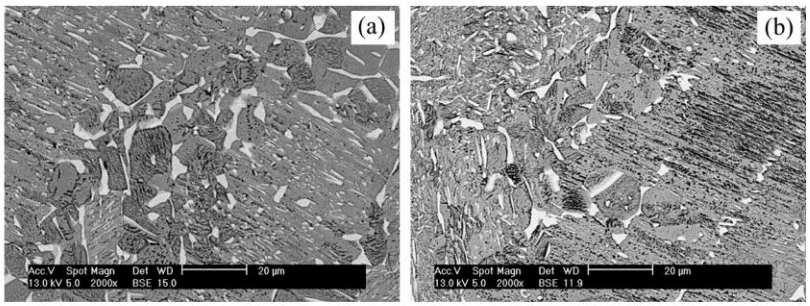

Fig.3 The BSE image of β-phase of two alloys in as-receive: (a) Ti-46Al-2Mo, (b) Ti-46Al-4Nb-2Mo

Fig. 5. Shows the microstructures of Ti-46Al-2Mo and Ti-46Al-4Nb-2Mo alloys after being heat-treated and water quench cooled. For the microstructure of the Ti-46Al-2Mo alloy (Fig. 5(a)), little patch clusters (dark regions) was seen on the bright α_2-massive matrix, implying that occasionally massive γ distribution occurred in the alloy. The water quenched microstructure of Ti-46Al-4Nb-2Mo alloy (Fig. 5(b)) was the same as the Ti-46Al-2Mo alloy microstructure, containing the massive γ structure (the dark areas) on the α_2-massive matrix (the white background) but the amount and the volume fraction (about 21pct) of γ-massive structure were lesser than that of the Ti-46Al-2Mo alloy. For fast cooling rate media by water quenching, one predominant property observed in all alloys is the presence of massive gamma grains (γ_m). The microstructure with increased transformation from α_2 phase to lamellae structure was obtained when 4Nb was added to Ti-46Al-2Mo alloy resulting in

Ti-46Al-4Nb-2Mo alloy. In the water quenched case, the microstructure Ti-46Al-2Mo microstructures, they exhibited massive γ phase on the α_2 phase matrix.

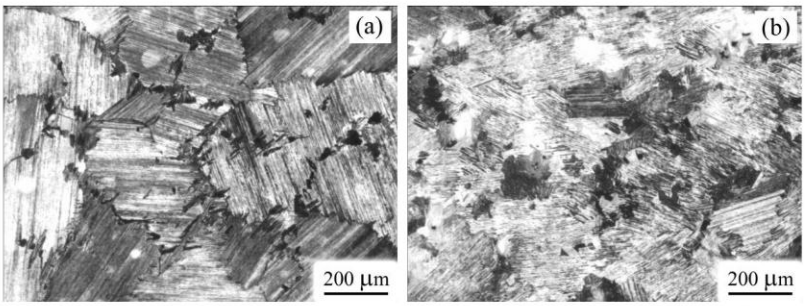

Fig.4 The microstructures of furnace cooled (a) Ti-46Al-2Mo, (b) Ti-46Al-4Nb-2Mo

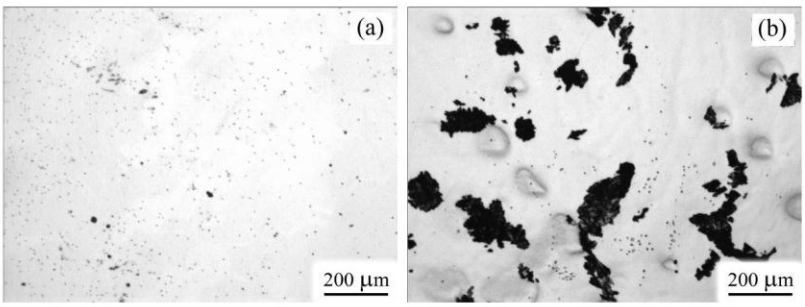

Fig.5 The microstructures of water quenched (a) Ti-46Al-2Mo, (b) Ti-46Al-4Nb-2Mo

An explanation of the transformation mechanism of γ_m structure is a set of massively (without composition change) formed γ grain initiated by grain boundary nucleation (mainly nucleating along triple junctions and grain boundary) in BOR with one of the two α-grains. Two possible nuclei which are twin related according to one of the crystallographic equivalent {111} planes such as $(111)_\gamma$ parallel to the habit plane $(0002)_\alpha$, are generated by this approach. Then, the next step is growth of massive grains in which the mechanism always proceeds by successive twining [7,8]. Prasad et al. [9] investigated the effects of Nb and Mn addition on the Ti-45Al based alloys and found that the massive transformation of gamma phase is most likely taken place by heterogeneous nucleation at the prior alpha grain boundaries before growing by short-range transferring of atoms across the incoherent interface. Earlier reports [10,11] have showed that fast cooling rate (such as OQ) is required to produce similar feather γ plate structures in both low Nb amount and high Nb amount alloys such as Ti-47-2Nb-2Cr and Ti-47Al-8Nb-2Cr. Similarly, the results in this study, (γ_f, i.e., one of the products obtained from massive transformation α→γ; massive γ, γ_m) also indicated that the cooling rate used to produce a given γ_m/ γ_f volume ratio in Ti-48Al-8Nb alloy is slower than that of the Ti-48 alloy [11]. Thus, this observation confirms that the Nb addition promotes the γ-massive transformation in the TiAl

alloy process.

Conclusion

The effects of alloying elements and cooling rates on the microstructures of Ti-46Al-2Mo and Ti-46Al-4Nb-2Moalloys have been investigated and the following conclusions have been drawn.

1. The solution treatment of casting alloys results in α_2/γ lamellae and small equiaxed microstructure of β phase. The changes of microstructure kinetics depend on the alloy chemistry and temperature.
2. The Nb and Mo addition can increase effect on morphological conformation of full lamellar and duplex structure. It was found that adding of Mo and Nb will decrease colony size of duplex structure and Mo adding results in increasing of lamellar transformation kinetic.
3. The slow cooling rates such as furnace or air cooling have significantly effect on fully lamellar transformation whereas the fast cooling, water quenching, results to increases of γ-massive transformation kinetic. Besides, Nb addition may also promote the massive transformation process.

Reference

[1] Kim Y-W., Wagner R., Yamaguchi M. 1995. Gamma titanium aluminides 1995. TMS Symposium Proceeding, Warrandale, PA; 637.

[2] X. H. Wu. 2006. Review of alloy and process development of TiAl alloys. *Intermetallics*. **Vol 14(10-11)**; 1114-1122.

[3] Appel F, Oehring M, Wangner R. 2000. Novel design concepts for gamma-base titanium aluminide alloys. *Intermetallics*. **Vol 8(9-11)**; 1283 -1312.

[4] G. Sreenivasulu, A.K. Singh, N.K. Mukhopadhyay, G.V.S. Sastry. 2005. Effect of alloying and aging on morphological changes from lamellar to equiaxed microstructure of $\alpha_2+\gamma$ titanium aluminides. *Metall Trans A* **Vol 36**; 2601-2613.

[5] R.M. Imayev, V.M. Imayev, M. Oehring, F. Appel. 2007. Alloy design concepts for refined gamma titanium aluminide based alloys. *Intermetallics* **Vol 15(4)**; 451-460.

[6] M. Kimura, K. Hashimoto. 1999. High-temperature phase equilibria in Ti-Al-Mo system. *J Phase Equi* **Vol 20**; 224-230.

[7] S.R. Dey, A. Hazotte, E. Bouzy. 2009. Crystallography and phase transformation mechanisms in TiAl-based alloys – A synthesis. *Intermetallics* **Vol 18(9)**; 1052-1064.

[8] A. Sankaran, E. Bouzy, J.J. Fundenberger, A. Hazotte. 2009. Texture and microstructure evolution during tempering of gamma-massive phase in a TiAl-based alloy. *Intermetallics* **Vol 17(12)**; 1007-1016.

[9] U. Prasad, M.C. Chaturvedi. 2003. Influence of Alloying Elements on the Kinetics of Massive Transformation in Gamma Titanium Aluminides. *Metall Trans A* **Vol 34**; 2053-2066.

[10] Y. Wang, J.N. Wang, Q.F. Xia, J. Yang. 2000. **Microstructure refinement of a TiAl alloy by beat treatment**. *J Mater Sci Eng A* **Vol (1-2)293** ;102-106.

[11] M. Takeyama, Y. Ohmura, M. Kikuchi, T. Matsuo. 1998. Phase equilibria and microstructural control of gamma TiAl based alloys. *Intermetallics* Vol 6(7-8); 643-646.

Appendix C

The influence of thermal processing on the microstructures of Ti-46Al(Nb, Cr) intermetallics alloys

Santirat Nansaarng and Panya Srichandr

Proceeding of the 7th International Materials Technology Conference and Exhibition,
IMTCE 2010 INOVATION FOR SUSTAINABILITY, 13-16 June 2010,
Hilton Kuching, Sarawak, Malaysia

The influence of thermal processing on the microstructures of Ti-46Al (Nb, Cr) intermetallics alloys

Santirat Nansaarng[1*] and Panya Srichandr[1]
[1]Division of Materials Technology, School of Energy, Environment and Materials
King Mongkut's University of Technology Thonburi, Bangkok 10140, Thailand.

Abstract

The effect of Nb and Cr addition on phase transformation of Ti-46Al-2Cr and Ti-46Al-4Nb-2Cr alloys during on differently cooling from α single phase field was investigated. The results indicated a very significant strong effect of Nb and Cr addition on decreased colonies size of microstructures and promoted the massive transformation by oil and water quenched.

Keywords: γ-TiAl, TiAl alloys; dual phase structures; alloying elements; heat treatment

Introduction

Titanium aluminides alloys with two-phase group ($\alpha_2+\gamma$) have long been considered to be suitable candidates for high temperatures structural application, since of their high specific strength, modulus, creep, excellent high temperature strength and good oxidation[1,2]. Chemical composition and thermal processing has strongly significant effects on microstructures and properties of TiAl-based alloys. In addition, Nb containing TiAl alloys is thought to be the potential high temperature structural due their low density, high melting points, and good elevated temperature strength and oxidation resistances [3], and previous research has show progress with simultaneous addition of substitutional elements such as Cr, Nb and Mo can improved high temperature strength and creep resistance, as well as room temperature ductility [4]. However, the thermal processing or heat treatment process can be to improve the microstructures and change properties of their TiAl. Indeed, varying the cooling rate from slow to fast can produce a range of microstructures including lamellar, Widmanstätten, feathery-like and/or massive microstructures [5]. This paper presents an investigation of effect of Nb and Cr addition on differently cooling transformation of Ti-46Al-2Cr and Ti-46Al-4Nb-2Cr alloys.

Experimental procedure

Two alloys used in this study, Ti-46Al-2Cr and Ti-46Al-4Nb-2Cr at.%, were prepared by non-consumable electrode arc melting. The button ingot weigh is 60g. The as-cast pancake shape samples were then cut by wire-electrical discharge machine prior to be subjected to solution treating. For solution treatment, the samples were soaked at the temperature of α single-phase area at 1400 °C for 30 min with air cooling (AC). Solution treated samples with a dimension of 10 mm ×10 mm ×10 mm were subsequently heat-treated at 1350 °C for 1 h before performing cooling step. Different kinds of media were utilized in the cooling, selecting based on cooling speeds as the lowest cooling rate by furnace cooling (FC), the intermediate cooling rate by air cooling (AC), and the fast cooling rate by oil quenching (OQ) and water quenching (WQ). All alloy samples that have been heat-treated were ground with SiC-based emery paper in order to remove the oxidized layer from the exposed surface before rinsing with water, then polishing to a 0.1 μm finish with diamond suspension, and etching by Kroll's reagent (5HF, 10mL HNO_3, and 85mL H_2O).

[1] **Santirat Nansaarng:** Corresponding author, E-mail :santirat.nan@kmutt.ac.th, Phone +662-470-8554-6, Fax +662-470-8557.

The microstructures and resultant phases of heat-treated samples were examined using X-ray diffraction (XRD), an optical microscope (OM) with Leica Q-Phase image analyzer, and a scanning electron microscope (SEM).

Results and Discussion

1. First step thermal processing

The XRD pattern of both alloys show the diffraction peak patterns indicated that the four alloys primarily consisted of the γ-TiAl phase with a minor amount of α_2-Ti_3Al phase and β phase (Fig. 1). The optical microstructures of two alloys solution treated at 1400 °C, 30 min, and air cooling are show in Fig. 2. The lamellar structure was found with a small volume fraction of equiaxed regions. The Ti-46Al-4Nb-2Cr alloy contained equiaxed microstructure more than the other three samples, as evidenced by the volume fraction of only around 20 pct. equiaxed structure. Since Nb stabilizes the β phase and thus, the maximum Al concentration for pure β solidification should be raised to a value above that the binary phase diagram, ie 44.7 at% Al [6].

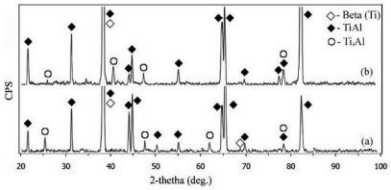

Fig. 1 XRD pattern of Ti-46Al-2Cr and Ti-46Al-4Nb-2Cr alloy

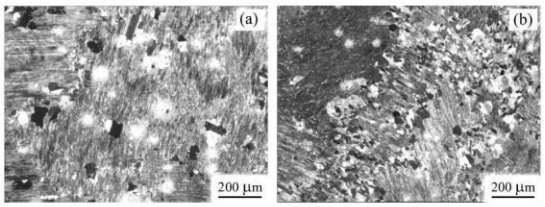

Fig. 2 Microstructures of Solution treated condition of Ti-46Al-2Cr and Ti-46Al-4Nb-2Cr alloy

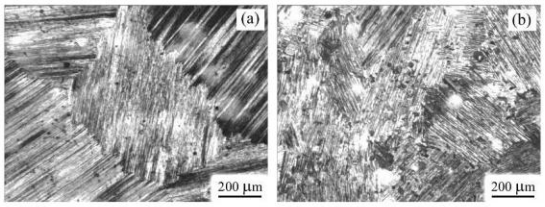

Fig. 3 Microstructures of furnace cooling condition of Ti-46Al-2Cr and Ti-46Al-4Nb-2Cr alloy

2. Microstructures resulting from various cooling rate

The slowest cooling rate received from using furnace, yielding the microstructures of the two alloys, Ti-46Al-2Cr, composing of coarse $\alpha_2 + \gamma$ lamellar grains with the grain size (GS) of about 200-600 μm. (Fig. 3(a)). The Ti-46Al-4Nb-2Cr alloy resulted in the decreases of $\alpha_2 + \gamma$ lamellar GS with GS at about 100 – 300 μm and occurrence of some equiaxed γ-monolithic grains (Fig. 3(b)).

The microstructures of the air cooled alloys are shown in Fig. 4. In case of Ti-46Al-2Cr alloy, the microstructure displayed fully lamellar structure with GS of approximately 200-500 μm (Fig. 4(a). Moreover, there was fine lath formation of γ phase arising at the edge of the grain boundary. The microstructutes of Ti-46Al-4Nb-2Cr (Fig. 4(b)) show the $\alpha_2 + \gamma$ lamellar grains with the Widmanstätten lath transformation at grain boundary and GS about 100-300μm and a lesser amount of the Widmanstätten lath transformation at grain boundary.

Fig. 5 show the microstructures of two alloys received from oil quenched. For the Ti-46Al-2Cr cases, as expected random distribution of few regions of massively transformed γ phase (dark regions, volume fraction about 10 pct.) were visible on the main α_2-bright matrix as can be seen in Fig. 5(a). In the micrographs, it is clearly that the microstructures of both alloys mostly exhibited the large α_2-massive grain amounts (α_{2m}) where they were transformed from the disorder α-phase (the diffusionless transformation above eutectoid temperature), and a lesser amount of γ-massive structure locating mainly at the grain boundaries with colony size of approximately 100-200 μm. The volume fraction of massively transformed γ phase was measured to be around 30pct. The Ti-46Al-4Nb-2Cr, where the micrograph is shown in Fig.5 (b). Apparently, the microstructure was large grains, and mainly consisted of the lamellar $\gamma+\alpha_2$ phase structure with large α_2-massive regions. The colony sizes were ranging from 350 to 500 μm. Transformation of this lamellar morphology started at the grain boundaries and grew into the grain interior. In a previous research [7], it has been conclusion that the feathery structure is metastable product resulted from no-equilibrium α to γ transformation which proceeds during cooling 1400 to1300 ^{o}C with small degree of undercooling in the Ti-48Al-3.5Cr alloy. The Widmanstätten structure forms starting at the temperature where the feathery structure formation ends. Although the formation mechanism of the feathery structure and the Widmanstätten structure are still controversial, many report [8,9] have firmly established that they are metastable products form at high temperature during continuous cooling from the α single phase field, and they can be preserved to room temperature only at intermediate cooling rate, such as air cooling and oil quenching.

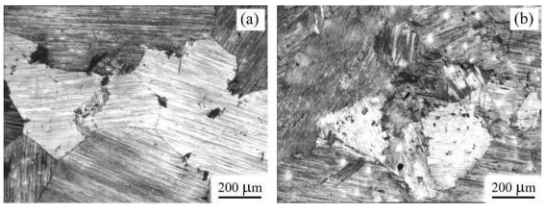

Fig. 4 Microstructures of air cooling condition of Ti-46Al-2Cr and Ti-46Al-4Nb-2Cr alloy

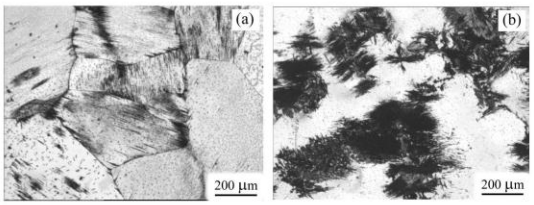

Fig. 5 Microstructures of oil quenched condition of Ti-46Al-2Cr and Ti-46Al-4Nb-2Cr alloy

The microstructures of two alloys from water quench were showed that Fig. 6. The Ti-46Al-2Cr microstructure had featureless bright α_2 matrix with fine acicular patches and about 15pct (dark regions)

volume fraction of massive γ structure (colony size at approximately 100-200 μm) (Fig. 6(a)). Ti-46Al-4Nb-2Cr alloy was illustrated in Fig. 6(b), showing that the microstructure composed of light and fine acicular patches of massive γ structure both inside the featureless bright α_{2m} matrix and at the α_{2m} grain boundary (colony size of about 30-200 μm). The volume fraction of the massive phase was about 12pct. (dark regions). In fact that Nb slow drowns the formation of feathery and lamellar microstructures implies that it may be related to their low diffusivity, but it has been shown that Nb is a slow diffuser in both TiAl and Ti_3Al with a diffusion coefficient about an order lower than Ti [10].

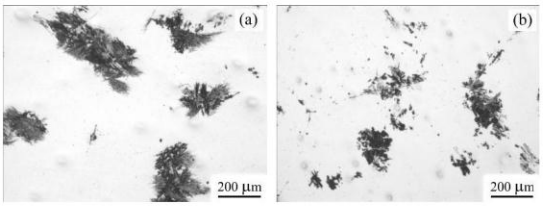

Fig. 6 Microstructures of water quenched condition of Ti-46Al-2Cr and Ti-46Al-4Nb-2Cr alloy

Conclusions

1. Addition of Nb and Cr into Ti-46Al alloy promote the formation of the γ-TiAl, α_2-Ti_3Al phase and β phase with fully lamellar and some equiaxed structure.
2. Nb and Cr can promote the α to γ_m massive transformation during oil and water quenching.
3. As Nb addition significantly decreases the colony lamellar grain size.

References

[1] X.J. Xu, L.H. Xu, J.P. Lin, Y.L. Wang, Z. Lin, G.L. Chen. 2005. Pilot processing and microstructure control of high Nb containing TiAl alloy. *Intermetallics* **Vol. 13**; 337-341.

[2] Z.X. Li, C.C. Cao. 2005. Effect of minor boron addition on phase transformation and properties of Ti-47.5Al-2Cr-2Nb alloy. *Intermetallics* **Vol 13**; 251-256.

[3] W. J. Zhang, S. C. Deevi, G. L. Chen. 2002. On the origin of superior high strength of Ti–45Al-10Nb alloys. *Intermetallics* **Vol 10**; 403-406.

[4] S.C Huang, E.L Hall. 1991. The effects of Cr additions to binary TiAl-base alloys. *Metall. Trans. A* **Vol 22**; 2619-2627.

[5] S.R. Dey, E. Bouzy, A. Hazotte. 2008. Features of feathery γ structure in a near-γ TiAl alloy. *Acta Mater. Vol 56*; 2051-2062.

[6] Ohnuma I., Fujita Y., Mitsui H., Ishikawa K., Kainuma R., Ishida K. 2000. Phase equilibrium in the TiAl binary system. *Acta Mater*. **Vol 48**; 3113-3123.

[7] E. Abe, K. Niinobe, M. Nobuki, M. Nakamura and T. Tsujimoyo In: E.P. George, M.J. Mills and M. Yamaguchi, Editors. 1991. High-temperature ordered-intermetallics alloys V, MRS, Pittsburgh (PA).

[8] M. Takeyama, T. Kumagai, M. Nakamura, M. Kikuchi, R. Darolia, J.J. Lewandowski, C.T. Liu, P.L. Martin and D.B. Miracle. 1993. Structural intermetallics, TMS, Warrendale (PA).

[9] G. Ramanath and V.K. Vasudevan In: I. Baker, R. Darolia and J.D. Whittenberger, Editors. 1993. High-temperature ordered-intermetallics alloys, MRS, Pittsburgh (PA).

[10] D. Hu, A.J. Huang, X. Wu. 2007. On the massive phase transformation regime in TiAl alloys: The alloying effect on massive/lamellar competition. *Intermetallics* **Vol 15**; 327-332.

Appendix D

Characterization of as-cast titanium aluminide on Ti-Al and Ti-Al-Nb system

Santirat Nansaarng and Panya Srichandr

WSEAS Transaction on Heat and Mass Transfer, 2006, Vol. 1, Issue 4, pp. 493-499

WSEAS TRANSACTIONS ON HEAT AND MASS TRANSFER Issue 4, Vol. 1, April 2006 ISSN: 1790-5044 493

Characterization of as-cast titanium aluminide on Ti-Al and Ti-Al-Nb systems

SANTIRAT NANSAARNG, PANYA SRICHANDR
King Mongkut's University of Technology Thonburi
126 Pracha-u-tid Rd., Bangmod Troong-kru, Bangkok 10140.
THAILAND
santirat.nan@kmutt.ac.th http://www.kmutt.ac.th

Abstract: - The investigation of Ti-Al and Ti-Al-Nb system with nominal composition of Ti–46Al, Ti–46Al-5Nb, Ti–46Al-10Nb, Ti–48Al, Ti–48Al–5Nb, and Ti–48Al–10Nb (at.%), were syntheses by arc melting under argon atmosphere. As-cast macrostructure and microstructure were studied on using optical microscopy, X-ray diffraction and scanning electron microscopy. Results showed that as-cast macrostructure of all alloys had dendritic structures exhibiting four-fold symmetry. The microstructures of Ti-46Al and Nb contents had lamellar colonies γ single phase and microstructure of Ti-48Al and Nb contents consisted of lamellar colonies of $\gamma+\alpha_2$ the β(B2) phase at grain boundary. Then found that the quantity of Nb in Ti-46Al and Nb contents had the influence of columnar dendrite and the high quantity of Nb in Ti-46Al and Nb contents also had effect to the disintegration of columnar dendrite into equixaed dendrite by Ti-46Al-10Nb would have a lot of equixaed dendrite and had the highest hardness value. Not only that Nb also affected to the lamellar colonies's quantity of γ single phase in Ti-46Al-10Nb that be increased more.

Key-Words: - Titanium aluminide, Intermetallics, TiAl, Phase transformation, Casting, Microstructure, Alloying elements

1 Introduction

Titanium aluminides and their composites are promising candidates as advanced structural materials for high temperature application because of their attractive combination of low density, oxidation resistance, high modulus, and strength retention at elevated temperatures [1-4]. They offer a significant weight-savings and similar mechanical performance characteristics compared to nickel superalloys, which can help attain weight-savings and cost reduction goals in future. TiAl base alloys of engineering interest usually are not in the composition range of single γ phase; a slightly off-stoichiometric composition on the Ti-rich side results in $\gamma+\alpha_2$ dual phase alloys. It has been shown that microstructure control, in addition to composition control, is the main factor to determine the strength of the TiAl alloys [5]. Usually, the near γ (NG) or duplex (DP) microstructures has superior tensile ductility at room temperature, but fracture toughness and high temperature strength are low. In contrast, the lamellar microstructure shows excellent strength and fracture toughness, with a low tensile ductility at room temperature. Recently, ternary TiAl–Nb alloys have also exhibited their capacity as potential high temperature structural materials [6]. Those alloys coincide with the conventional TiAl alloys characterized as low density, simple lattice. However, gaining the optimal mechanical properties and excavating abundantly the ternary TiAl–Nb alloys' potential mainly needs fine microstructures of these alloys [7]. There are two methods of obtaining the fine grains, including conventional thermo-mechanical processing and alloying. Zhang et al. [8] has reported that the Nb addition of 5–10 at.% can significantly improve the strength of TiAl-base alloys. The origin of this strengthening effect is not altogether clear. It may arise from solid solution as has been suggested by Zhang et al. [8]. Alloying with Nb often leads to a refinement of the microstructure, as has been recognized in [9]. Thus, the strengthening effect may in terms of a Hall–Petch mechanism be attributed to dislocation interactions with internal boundaries [9]. Another hypothesis is that additions of Nb lead to a decrease of the stacking fault energy. This paper investigated systematically the effects of Nb and Al contents on the microstructure and properties. What is the difference between the effects of these two alloying additions? The detailed macrostructure and microstructures of Nb in the TiAl alloys will be reported in a separated paper.

2 Experimental procedure

TiAl based alloys with norminal composition (at.%) of Ti-46Al , Ti-48Al, Ti-46Al-5Nb, Ti-48Al-5Nb, Ti-46Al-10Nb and Ti-48Al-10Nb were used in this study. The alloys were prepared as 60g buttons from high purity Ti (99.9%), Nb (99.98%) and Al (99.98%) (Fig.1.) by arc melting in argon atmosphere in a water-cooled copper hearth. The buttons were remelted 5-6 times to ensure chemical homogeneity. The nominal compositions were taken as weight loss after melting did not exceed 0.5%. The macrostructure of dendrite morphology was observed at the top surface without etching. The cast microstructure was studied using the cross-sections of the top side of button-shaped ingot.

The macrostructure, microstructure and phases presented in the alloys were studied by using optical microscopy (OM) with Leica images analyzer, scanning electron microscopy (SEM) and X-Ray diffraction (XRD). The samples for OM were etched in a solution of modified Kroll's reagent (5% HF, 15% HNO_3, 80% H_2O).

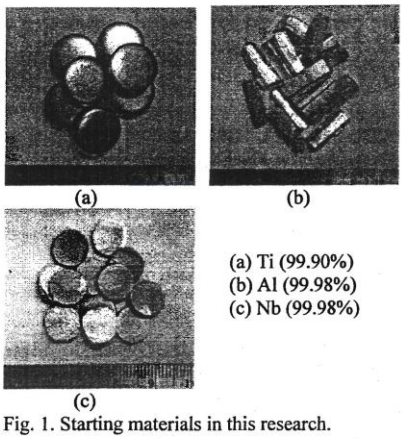

Fig. 1. Starting materials in this research.

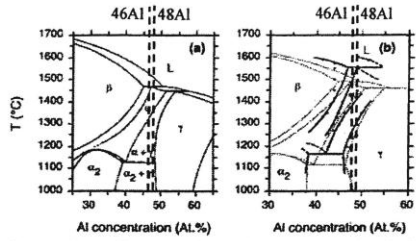

Fig. 2. Phase diagram of (a) Ti-Al and (b) Ti-Al-Nb system [11]

3 Results and Discussion

3.1 As-cast macrostructure

Macrostructure at the top surface of button-shaped specimens of Ti-Al and Ti-Al-Nb alloys(Fig. 3) have same macro and microstructure because when Nb concentration not more than 15%Nb, phase combinations are the same as for binary alloys[10].

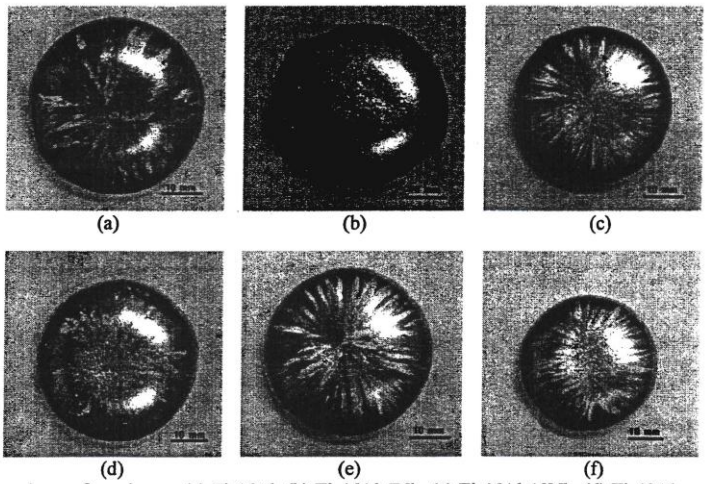

Fig. 3. Button shape of specimens. (a) Ti-46Al; (b) Ti-46Al-5Nb; (c) Ti-46Al-10Nb; (d) Ti-48Al; (e) Ti-48Al-5Nb; (f) Ti-48Al-10Nb

WSEAS TRANSACTIONS ON HEAT AND MASS TRANSFER Issue 4, Vol. 1, April 2006 ISSN: 1790-5044

There alloys was reveals that the primary solidification path shift from L→α, α→α+γ and α+γ→α_2+γ phase with all Al and Nb content (Fig.2). Solidification structures are dendritic at all compositions. The six alloys consist of dendritic structures exhibiting four-fold symmetry [(Fig. 4(a)-(d)]. The alloys structure on Ti-Al system will have dendrite structure features which had big size and show out in four–fold symmetry features. But when compared with the case of Ti-Nb Alloys system which find that dendrite feature would have similar features smaller but the dendrite cell

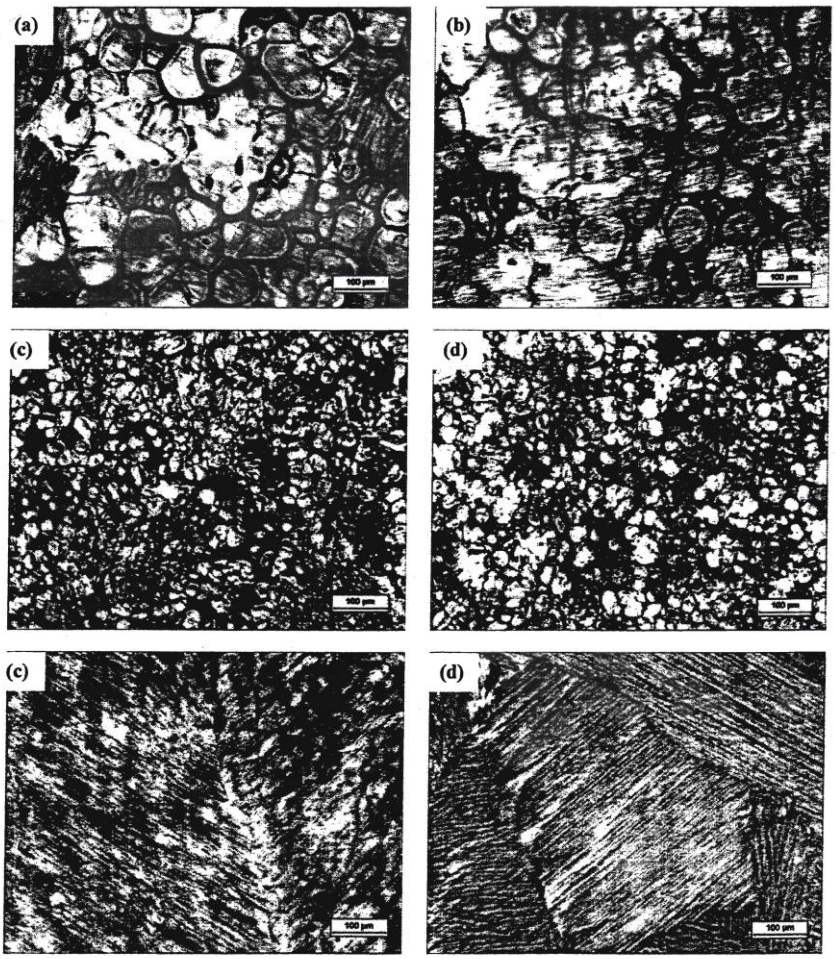

Fig. 4. Optical micrographs viewing the top surface (a)-(d) and microstructure of cross-section (e), (f), which illustrate various dendrite structure and microstructure depending on the composition of alloys. (a) Ti-46Al; (b) Ti-48Al; (c) Ti-46Al-10Nb and (d) Ti-48Al-10Nb; (e) Ti-46Al; (f) Ti-46Al-10Nb (all in at%).

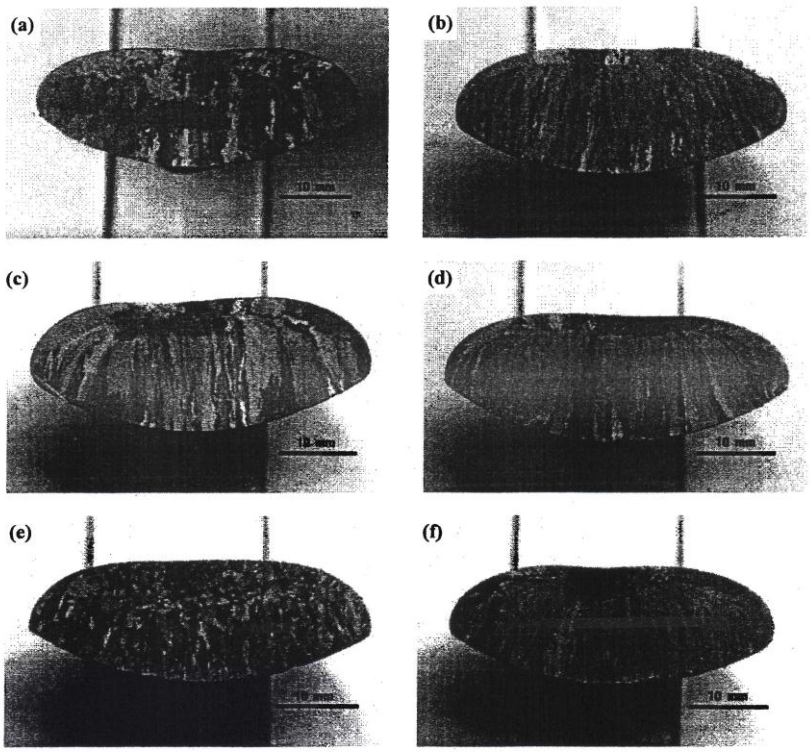

Fig. 5. Partially melted arc-melt ingots. (a) Ti-46Al; (b) Ti-48Al; (c) Ti-46Al-5Nb; (d) Ti-48Al-5Nb; (e) Ti-46Al-10Nb; (f) Ti-48Al-10Nb.

features were smaller. When decreased the A1 quantity and increased Nb quantity would make dendrite cell size smaller, according to this experiment: Ti-46A1-10Nb had the smallest dendrite cell size. When considered the button directional solidification features found that the frozen was almost columnar structure by the directional solidification would thrust from beneath to the top of button middle surrounding and also occurred shrinkage on them. When considered the relation of A1 and Nb quantities in Ti found that Ti-46A1 in alloys when Nb quantity had more increasing would make the changing of solidification structure features by would make the columnar structure was decreased and had the features of equiaxed structure occurred which started to find when filled Nb in 5% and equiaxed structure would have smaller size (Fig.5). When added the Nb quantity in 10% (Ti-46A1-10Nb) which the composition that occurred the spread of structure and was the smallest grain composition. For Ti-48A1 alloy group found that Nb quantity which filled not had more effective by didn't make the solidification features be changed which was still the columnar structure, only if the secondary dendrite features had smaller size by the Ti-48A1-10Nb composition had the most dedicated secondary dendrite.

3.2 X-ray diffraction analysis

Fig. 7-8 shows the X-ray diffraction pattern of Ti-16Al, Ti-46Al-10Nb and Ti-48Al-10Nb of as-cast structures. Result of the analysis with x-ray diffraction pattern of Ti-46Al, Ti-46Al-10Nb and Ti-48Al-10Nb found that alloys pattern Ti-46Al and Ti-46Al-10Nb had same features by the

patterns were specified that in as-cast structure had Single crystal structure which is γ-TiAl only and in alloys Ti-48Al-10Nb had three crystal structure patterns which are γ-TiAl, α_2-Ti_3Al and B2.

3.3 As-cast microstructure

After being as-cast and left it cooled in copper-water cooled mould ready, Ti-46Al, Ti-46Al-5Nb and Ti-46Al-10Nb found that got the microstructure in full lamellar pattern of γ-TiAl (Fig. 6) that considered from quantity of alloying elements which filled in and showed that quantity of Nb didn't have any effect to structure occurring because from the past researches found that if quantity of Nb lower than 15% in alloys with composition of Al<48(%at.) didn't have any effect to new structure occurring[10] and Nb also had effect to lattice parameter of γ-TiAl because quantity of Nb which filled in would be effect to

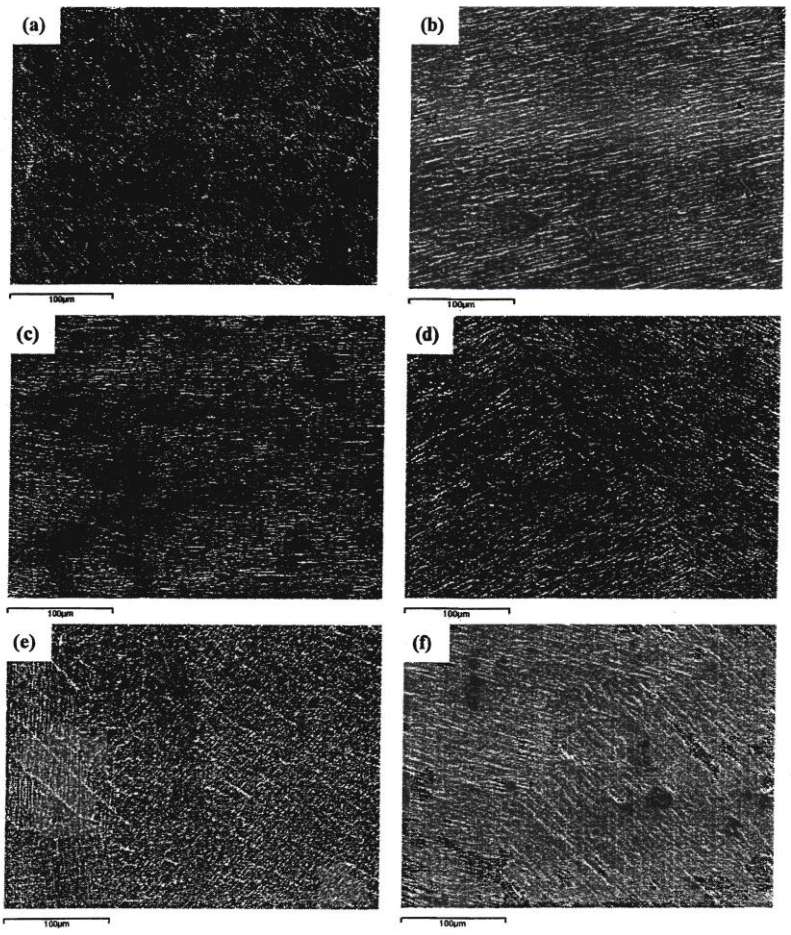

Fig. 6. SEM photographs of typical microstructure of Ti-Al and Ti-Al-Nb alloys. (a) Ti-46Al; (b) Ti-46Al-5Nb; (c) Ti-46Al-10Nb; (d) Ti-48Al; (e) Ti-48Al-5Nb; (f) Ti-48Al-10Nb.

increased c-axis but a-axes didn't had any effect because Nb would be in place of Ti. When the quantity of concentration of Al in alloy with constantly, the above-mentioned behaviour was considered to arise from substituting Nb for Ti of the γ-TiAl single phase. [10], [12] Moreover when the quantity of Nb increased would be effected to the lamellar size which smaller. The result of Z.C. Liu et al. research [13] found that the quantity of Nb which increased while Al decreased would be affected to lamellar spacing (λ) that had smaller size but for alloys Ti-48Al would had 3 phases which were γ-TiAl, α_2-Ti_3Al and B2. From this result volume faction of γ-TiAl would be more than α_2-Ti_3Al and B2 in priority and when increased the quantity of Nb to 10% showed that had the difference of lamellar size to be in smaller size and also made the volume fraction of α_2-Ti_3A to be increased more.

3.3 Hardness

Fig. 9. present Vickers hardness for each binary and ternary composition. The value of alloy's hardness was found that when considered from the combination image, the value of hardness would be affected to the hardness value. It means that in the-vicinity but when considered from 2 alloys groups: Ti-46Al+Nb and Ti-48Al+Nb was found that the quantity of Nb in Ti-46Al+Nb group would when increased more the quantity of Nb, the hardness value would be increased along too. On the highest hardness value in alloy Ti-46Al-10Nb at 269.67 HV but when considered Ti-48Al+Nb group was found that the average of hardness value of 3 parts had be in the vicinity: 186.33(Ti-48Al), 185.73(Ti-48Al-5Nb) and 186.00(Ti-48Al-10Nb) in orderly. So the quantity of Nb which filled in alloy Ti-48Al group didn't effect to the hardness value.

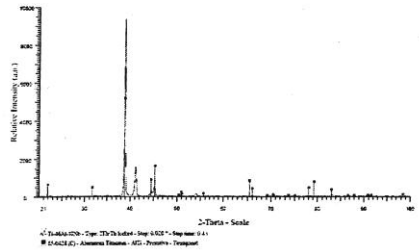

Fig. 7. XRD pattern of Ti-46Al-10Nb

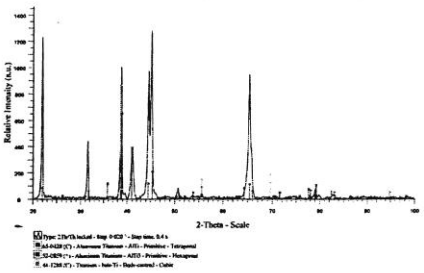

Fig. 8. XRD pattern of Ti-48Al-10Nb

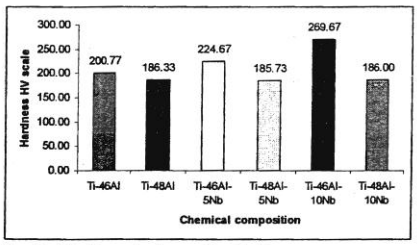

Fig. 9. Hardness test results of alloys

4 Conclusions

For this work the following conclusions are with drawn:

1. as-cast structures of arc-melt Ti-46Al+Nb and Ti-48Al+Nb present strong microsegragation, revealed by the systematic occurrence of interdendritic γ-TiAl phase;
2. the Nb addition to the Ti-46 alloy are favorable to the as-cast structures γ-TiAl single phase. The effect of the 10Nb addition is even more excellent for the as-cast lamellar structure stability at room temperature and has highness hardness value;
3. as-cast structures of Ti-48Al+Nb alloy has duplex lamellar of γ-TiAl + α_2-Ti_3Al and β(B2) phase.

References:

[1] Appel, F., et al., Recent Progress in the Development of Gamma Titanium Aluminide Alloys, *Advanced Engineering Materials*, Vol.11, No. 2, 2000, pp. 699-720

[2] Appel, F. and R. Wagner, Microstructure and Deformation of Two-Phase Gamma Titanium Aluminides, *Materials Science and Engineering A*, Vol. 22, No. 5, 1998, pp. 187-268.

[3] Clemens, H. and H. Kestler, Processing and Applications of Intermetallic γ-TiAl Based Alloys, *Advanced Engineering Materials*, Vol. 9, No. 2, 2000, pp. 551-570

[4] Lipsitt, H.A., Titanium Aluminides - An Overview, *Material Resource Society Symposium Proceedings*, Vol. 39, 1985, pp. 351-364

[5] Guoliang Chen, Zuqing Sun and Xing Zhou, Oxidation and mechanical behavior of intermetallic alloys in the Ti---Nb---Al ternary system, *Materials Science and Engineering: A*, Vol. 153, No. 1-2, pp. 597-601.

[6] J. G. Wang, L. C. Zhang, G. L. Chen and H. Q. Ye, Formation of stress-induced 9R structure in a hot-deformed Ti-45Al-10Nb alloy, *Scripta Materialia*, Vol. 37, No. 2, pp. 135-140.

[7] Q . Hong, L. Zhou, G.Z. Luo et al., *Proceeding of the Xi' an Interconference Titanium Conference, September 15-18, 1998, Xi' an, Chaina*, 1998, pp. 1019-1024.

[8] W.J. Zhang, Z.C. Liu, G.L. Chen, Y.W. Kim, Deformation mechanisms in a high-Nb containing γ–TiAl alloy at 900°C , *Materials Science and Engineering: A*, Vol. 271, No. 1-2, 1999, pp. 416-423.

[9] J.D.H. Paul, F. Appel, R. Wagner, The compression behaviour of niobium alloyed γ-titanium alumindies, *Acta Materialia*, Vol. 46, No. 46, 1998, pp. 1075-1085.

[10] Toshimitsu Tetsui, Effects of brazing filler on properties of brazed joints between TiAl and metallic materials, *Intermetallics,* Vol. 9, No. 3, 2001, pp. 253-260.

[11] J. H. Westbrook., *Intermetallic Compound, Structure Application of Intermetallic Compound*, John Wiley & Sons, 2000, pp.75

[12] Chen GL, Zhang WJ, Liu ZC, Li SJ, Kim Y-W, Gamma titanium aluminides, *TMS*, 1999, pp. 371.

[13] Z.C. Liu , J.P. Lin, S.J. Li, G.L. Chen, Effects of Nb and Al on the microstructures and mechanical properties of high Nb containing TiAl base alloys, *Intermetallics*, Vol. 10, 2002, pp. 635-659.

Appendix E

Synthesis of intermetallic compound of Ti-Al and Ti-Al-Nb system and their properties

Santirat Nansaarng and Panya Srichandr

Proceeding of the 4th WSEAS International conference on Heat Transfer, Thermal Engineering and Environment, Elounda, Greece, August 21-23, pp.254-257

Proceedings of the 4th WSEAS Int. Conf. on HEAT TRANSFER, THERMAL ENGINEERING and ENVIRONMENT, Elounda, Greece, August 21-23, 2006 (pp254-257)

Synthesis of intermetallic compounds of Ti-Al and Ti-Al-Nb systems and their properties

SANTIRAT NANSAARNG, PANYA SRICHANDR
King Mongkut's University of Technology Thonburi
126 Pracha-u-tid Rd., Bangmod Troong-kru Bangkok. 10140.
THAILAND
santirat.nan@kmutt.ac.th http://www.kmutt.ac.th

Abstract: - As-cast microstructure of Ti-Al and Ti-Al-Nb system with nominal composition of Ti–45Al, Ti–48Al, Ti–45Al-5Nb, Ti–48Al–5Nb, Ti–45Al–10Nb, and Ti–48Al–10Nb (at.%), were syntheses by arc melting under argon atmosphere. The morphology, distribution and dendrite cell size of an as-cast Ti-Al and high Nb containing TiAl alloys had been investigated. The results showed that as-cast structures of Ti-Al and Ti-Al-Nb were presented strong microsegregations. The dendrite cell size of Ti-Al binary alloys was found that decreases on decreasing Al content. The Nb contents had influence to dendrite cells and phase formations of Ti-Al-Nb ternary alloys, which the Ti-45Al-10Nb (at%.) were found minimize dendrite cell size and strong single γ-TiAl phase.

Key-Words: - Titanium aluminide, Intermetallic compound, TiAl, Phase transformation, Casting, Microstructure, As-cast structure.

1 Introduction

The TiAl intermetallic compound is an attractive material for high-temperature structural applications because of its low density, high melting point and high specific strength at elevated temperature and good oxidation resistance [1-3]. The titanium aluminides family is composed of three main compounds as followed as: the first group was Ti_3Al also designated as α_2-phase orders according to $D0_{19}$ structure with a hexagonal symmetry and of lattice parameters a or $d = 2a$ disor = 0.58 nm; c or $d = 0.48$ nm. The latter derives from A3 type structure but presents a long range order only in the direction perpendicular to the c-axis. The second group was TiAl (noted γ) ordered up to the melting point has an $L1_0$ type face-centered tetragonal structure consisting of atomic layers perpendicular to the c-axis and the last group was $TiAl_3$ orders according to the $D0_{22}$ structure. This structure is related to two $L1_2$ type unit cells stacked along the c-axis with an antiphase boundary of 1/2 [1 1 0](0 0 1) type at every other (0 0 1) plane[4].

The TiAl base alloys of engineering interest usually is not in the composition range of single γ phase; a slightly off-stoichiometric composition on the Ti-rich side results in $\gamma + \alpha_2$ dual phase alloys. It has been shown that microstructure control, in addition to composition control, is the main factor to determine the strength of the TiAl alloys [5,6]. Usually, the near gamma (NG) or duplex (DP) microstructures has superior tensile ductility at room temperature, but fracture toughness and high temperature strength are low. In contrast, the lamellar microstructure shows excellent strength and fracture toughness, with a low tensile ductility at room temperature [7].

The properties of TiAl alloys are strongly composition and microstructure dependent. Alloying elements dominate the strengths of alloys for given microstructures. Al is the most influential element to the alloy strength and it acts through changing the volume fraction of the α_2 phase, which is the hard phase in $\alpha_2 + \gamma$ two phase alloys. With a decrease in Al concentration the α_2 volume fraction is increased and so is the strength. Other elements like Nb seem not to have as large an effect on alloy strengths through solid solution up to a certain temperature [8]. However, elements like Nb, W, Ta, Hf can influence the kinetics of phase transformation and greatly improve the oxidation and creep resistance [9]. Such elements, especially Nb, have been added frequently into TiAl-based alloys. This paper investigated systematically the effects of Nb and Al contents on the dendrite morphology and alloys phases of Ti-Al and Ti-Al-Nb system.

2 Experiments

Small ingots of six alloys buttons (~60g) from high purity Ti (99.9%), Nb (99.98%) and Al (99.98%) with nominal compositions (in atomic fraction) of Ti–45Al, Ti–48Al, Ti–45Al-5Nb, Ti–48Al–5Nb, Ti–45Al–10Nb, Ti–48Al–10Nb were

Proceedings of the 4th WSEAS Int. Conf. on HEAT TRANSFER, THERMAL ENGINEERING and ENVIRONMENT, Elounda, Greece, August 21-23, 2006 (pp254-257)

produced by non-consumable electrode argon arc melting with a water-cooled copper mold in an atmosphere of argon. Each ingot was remelted five times to ensure complete mixing of the constituents and homogeneity. The nominal compositions were taken as weight loss after melting

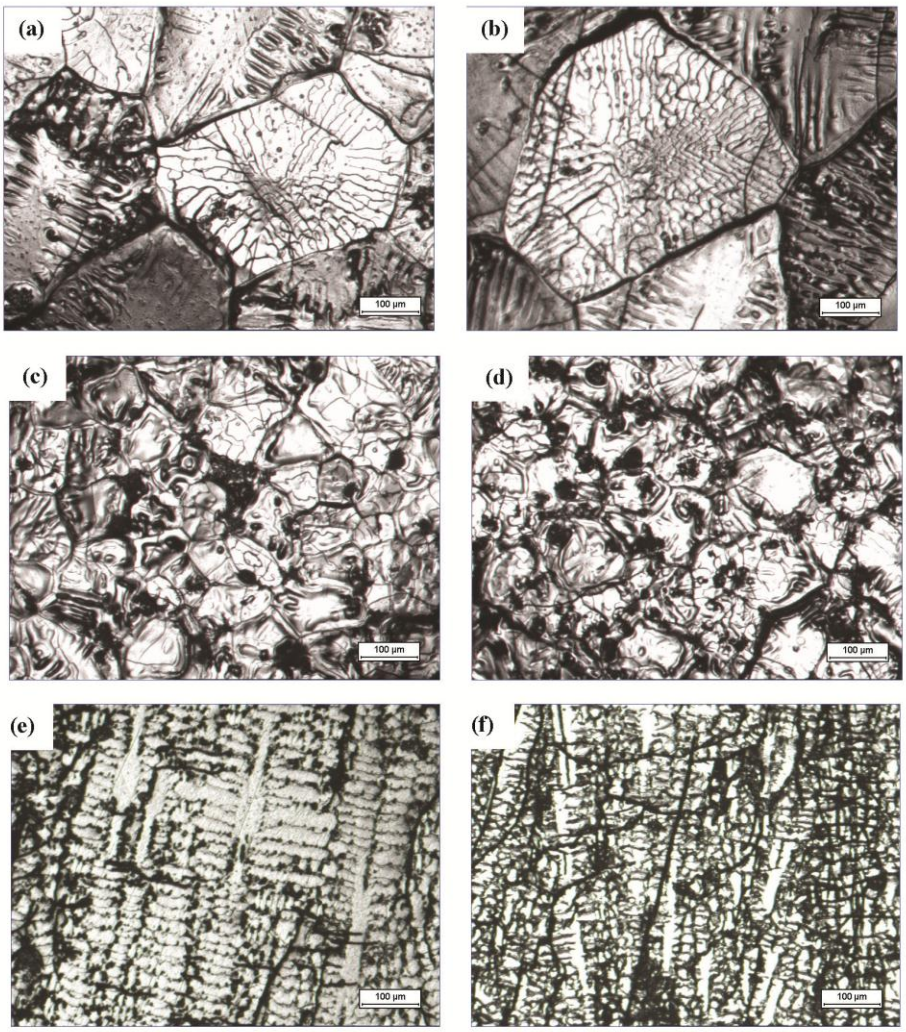

Figure 1. Optical micrographs viewing the top surface (a)-(d) and cross-section (e), (f), which illustrate various dendrite structure depending on the composition of alloys: (a) Ti-45Al; (b) Ti-48Al; (c) Ti-45Al-10Nb and (d) Ti-48Al-10Nb; (e) Ti-45Al; (f) Ti-45Al-10Nb (all in at%).

did not exceed 0.5%. The alloy bottom side of a button-shaped ingot showed columnar structure since it directly contacts with water-cooled Cu mold. Only a small portion of top side (about 1/5 of its height) showed more or less equiaxed dendrite microstructure. The macrostructure of dendrite

Proceedings of the 4th WSEAS Int. Conf. on HEAT TRANSFER, THERMAL ENGINEERING and ENVIRONMENT, Elounda, Greece, August 21-23, 2006 (pp254-257)

morphology was observed at the top surface without etching. The cast microstructure was studied using the cross-sections of the top side of button-shaped ingot. The etching solution used was Kroll's reagent (5% HF, 15% HNO_3, 80% H_2O) [10].

The phase identification and microstructure of the as-cast specimen was observed with a Bruker D8 Advance X-Ray Diffractometer (XRD) and Optical microscopy (OM) with Leica images analyzer.

3 Research results

Fig. 1. shows the morphology of top surface of button-shape ingot of Ti-Al and Ti-Al-Nb compounds reveals that primary solidification. Solidification structures are dendrite at all Al and Nb contents. The compounds containing Al only and Al-Nb consist of dendrite structure exhibiting four-fold symmetry [Fig.1 (a), (b), (c) and (d)]. This is also confirmed in optical microstructures of etched cross-section of button specimens as exemplified in a 45 at% Al and 45 at%-10at%Nb alloys [Fig. 1. (e) and (f)].The cell size of dendrite structure was observed to greatly vary with Al and Nb contents.

Fig. 2. shows the relationship between alloying elements (Nb and Al) and dendrite cell size in the six series of alloys. It can be seen that dendrite cell size (DCS) decreases with a decrease in Al content for two alloys of Ti-Al system. The Ti-45Al alloy has DCS minimize about 436.10μm. The variations of Nb and Al in the Ti-Al-Nb ternary alloys seem similar to that in the Ti-Al binary alloys from Fig. 2, but the dendrite cell size decreases with increases in Nb content. The Ti-45Al-10Nb has minimized of DCS about 314.59 μm.

The XRD pattern obtained from the minimize dendrite cell size specimen is given in Fig. 3. It demonstrates that in the Ti-Al-Nb alloys, which Nb has more effect of γ phase. It was identified to be single phase γ-TiAl. For Ti-45Al-10Nb (at%.) alloy is in agreement with Ding and Hao's paper [11]. We have referred to many Ti-Al-Nb ternary phase diagrams available in the literature. However, most of the Ti-Al-Nb ternary phase diagrams available are very different. The TiAl-Nb diagram needs further systematic investigation.

4 Conclusion

For the Ti-Al binary alloy and Ti-Al-Nb ternary alloy. On the basis of above investigation on the influence of Al and Nb contents on dendrite cell size and phase content, the following conclusions were obtained:

(1) The presence of minimize of dendrite cell size of two Ti-Al binary alloys, appear to decrease Al content.

(2) Among of four Ti-Al-Nb ternary alloys investigated in this study, the single phaseγ-TiAl has found in higher Nb content, but lower Al content.

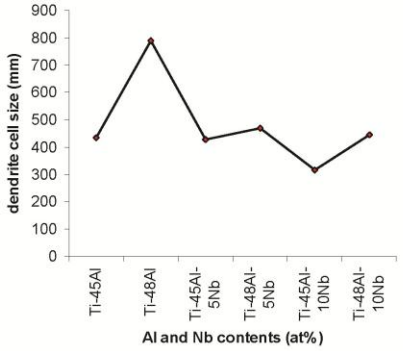

Figure 2. Variation of dendrite cell size as function of Al and Nb contents.

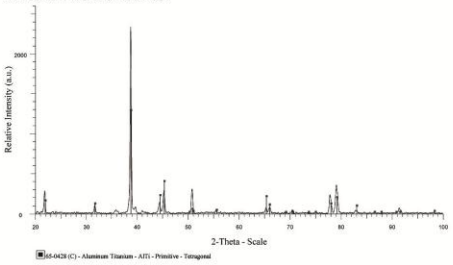

Figure 3. X-Ray diffraction spectrum obtained for Ti-45Al-10Nb alloys. Existence of strong γ phase.

References

[1] Kim YW, Dimiduk DM. In: Nathal MV, Darolia R, Liu CT, Martin PL, Miracle DB, Wagner R, et al., editors. *Structural intermetallics II*. TMS; 1997. p. 531.

[2] Takeyama M. Mater Sci Eng 1992;A152:269.

[3] Tsuyama S, Mitao S, Minakawa K. In Kim Y-W, Boyer RR, (editors).*Microstructure/ property relationships in titanium aluminides and alloys*. Warrendale (PA): TMS: 1991. p 213.

[4] S. Djanarthany et al.,*Materials Chemistry And Physics 72*., 2001., p305.

Proceedings of the 4th WSEAS Int. Conf. on HEAT TRANSFER, THERMAL ENGINEERING and ENVIRONMENT, Elounda, Greece, August 21-23, 2006 (pp254-257)

[5] Kim YM. In: Kim YM, Wagner R, Yamaguchi M, editors. *Gamma titanium aluminides*. TMS; 1995, p. 637.
[6] Kim YM. *Mater Sci Eng* 1995;A192/ 193:519.
[7] Z.C. Liu, J.P. Lin, S.J. Li, G.L. Chen, *Intermetallics 10*, 2002, p. 653
[8] Appel F, Lorenz U, Paul JDH, Oehring M. In: Kim Y-W, Dimiduk DM, Loretto MH, editors. *Gamma titanium aluminides* 1999. Warrendale, (PA): TMS, 1999. p. 381.
[9] Huang S-C. In: Darolia R, Lewandowski JJ, Liu CT, Martin PL, Miracle DB, Nathal MV, editors.*Structural intermetallics*. Warrendale (PA): TMS, 1993. p. 299.
[10] Gunter Petzow., *Metallographic Etching*, 2nd edition, 1999, ASM International., p. 142.
[11] Jin-Jun Ding and Shi-Ming Hao, *Intermetallics 6*, 1998, p. 329